Applications of a high-order algorithm for LES and CAA in complex geometries

Frédéric Daude, Julien Berland, Philippe Lafon, Fabien Crouzet, Christophe Bailly

Applications of a high-order algorithm for LES and CAA in complex geometries

F. DAUDE[a], J. BERLAND[a], P. LAFON[a,b], F. CROUZET[b] AND C. BAILLY[c]

a. LaMSID, 1 av. du Général De Gaulle, 92141 CLAMART (FRANCE)
b. EDF R&D, 1 av. du Général De Gaulle, 92141 CLAMART (FRANCE)
c. LMFA, 36 av. Guy de Collongue, 69134 ECULLY (FRANCE)
& Institut Universitaire de France

Abstract :

High sound pressure levels are produced by non-linear interactions between acoustics and aerodynamics in confined flows. To tackle these couplings, a numerical tool called Code_Safari has been developed. The solver is based on optimized high-order finite-difference schemes combined with optimized filters on a multi-domain approach. In addition, a shock-capturing filter has been implemented to deal with compressible flows. This solver has been validated on classical test problems and key results obtained for three realistic applications, namely noise generated by ducted cavity, sudden enlargement and by rod-airfoil interaction, are reported.

Key words: Large-Eddy Simulation, Computational AeroAcoustics

1 Introduction

Large-Eddy Simulation (LES) of turbulence needs to accurately resolve a wide range of length scales. This is specially the case for the direct computation of aerodynamic noise for which a high disparity is found between the turbulent flow and the radiated acoustic field [1]. This requires the use of numerical methods with minimal dissipation and dispersion errors. The implicit compact [2] or the explicit DRP [3] or optimized [4] finite-difference schemes in conjunction with selective filter are an attractive choice for LES in order to reduce both amplitude and phase numerical errors. The generalized coordinates approach [5, 6] is used in the present work as well as an overset-grid strategy and a high-order interpolation for the communication between non-coincident grids [7, 8, 9]. Moreover, high-speed flows are characterized by shock wave/turbulence interactions. To correctly describe discontinuities in compressible turbulent flows, a shock-capturing procedure must also be used. This method is however often highly dissipative [10] and the use of adaptive shock-capturing filters with efficient discontinuity sensors allows to minimize this effect [11, 12]. A numerical tool called *Code_Safari* [13] has been previously developed and validated using such numerical procedures. The present paper deals with the application of this solver of fluid dynamics equations on realistic configurations characterized by complex aeroacoustic couplings.

2 Governing equations and numerical procedure

The three-dimensional Navier-Stokes equations expressed in a general body-fitted curvilinear coordinates are written in the following strong conservative form:

$$\partial_\tau \hat{U} + \partial_\xi \left(F_\xi - F_\xi^\nu\right) + \partial_\eta \left(F_\eta - F_\eta^\nu\right) + \partial_\zeta \left(F_\zeta - F_\zeta^\nu\right) = 0 \tag{1}$$

where τ is the time, ξ, η and ζ the computational coordinates. $\hat{U} = U/J$ where U is the vector of conservative variables and J the Jacobian of the coordinate transformation between Cartesian and computational coordinates. F_ξ, F_η, F_ζ are the inviscid flux-vectors and $F_\xi^\nu, F_\eta^\nu, F_\zeta^\nu$ the viscous flux-vectors. The spatial derivatives in equation (1) are approximated using a 11-point optimized finite-difference scheme in conjunction with a low-pass filter [4]. In particular, the classical explicit second-order accurate four-stage Runge-Kutta is used for the time advancement. To correctly capture discontinuities in compressible flows, a self-adaptive artificial dissipation model is applied via a non-linear filter at each time step. To tackle complex geometries, an overset-grid approach with high-order explicit non-optimized Lagrangian interpolation is used. Detailed description and numerical validations of this high-order algorithm may be found in Ref. [13].
The selective filter used to improve the numerical stability of the non-dissipative spatial discretization is also used to separate the large scales from the small ones. This filter takes into account the dissipative effects of the subgrid scales by draining energy at the cut-off frequency. The selective filter leaves flow features larger

than the cut-off wavelengths unaffected, while properly removing the energy being transferred to smaller wave lengths. Interactions between the resolved and the unresolved scales are however neglected. This LES based on relaxation filtering (LES-RF) approach has already been performed in round jets [14] and cavity flows [15] among others.
The aforementioned features of the numerical algorithm are embodied in the parallel time-accurate code *Code_Safari* [13]. In the following, some important results are addressed on realistic configurations with industrial relevance and LES computations are performed to highlight complex aeroacoustic couplings.

3 LES of low-speed flow past a ducted cavity

It is well established that compressible flows past open cavities cause high levels of pressure fluctuations. Many experimental and numerical investigations were performed to understand the underlying physical mechanism and develop efficient control strategy, see Ref. [16] for a review. The self-sustained cavity oscillations are due to a complex feedback mechanism between the upstream and downstream corners which is referred to as cavity (or Rossiter) modes (RM). The corresponding frequencies are given by the semi-empirical formula, proposed by Rossiter [17]:

$$St_R = \frac{f_{n_R} d}{u} = \frac{n_R - \alpha}{M + 1/\kappa} \tag{2}$$

in which u and M are the external flow velocity and Mach number respectively, d is the cavity length, n_R is the mode number. The two empirical constants α and κ are linked to the delay between the vortex impact and the acoustic wave emission and the convection velocity of vortices in the shear layer. Developing effective control strategy and understanding the underlying physical mechanism of the cavity noise reduction is still a research area, refer to Refs. [18, 19].

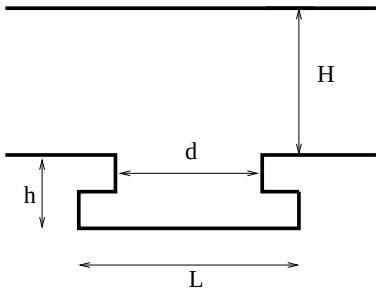

Figure 1: Ducted cavity: sketch of the geometry; $d = 0.05$ m, $h = 0.02$ m, $H = 0.137$ m, $L = 0.073$ m.

For ducted cavities, the cavity modes can be coupled with duct acoustic modes which can lead to high amplitude oscillations even at low speed. Such configurations can be found in pipe systems with flow control devices such as valves, in organ pipes or in flutes, for instance. The frequencies of the duct transverse mode (DM) are given by:

$$St_D = \frac{f_{n_D} d}{U} = \frac{n_D d}{2HM} \tag{3}$$

in which H is the height of the duct and n_D is the mode number.

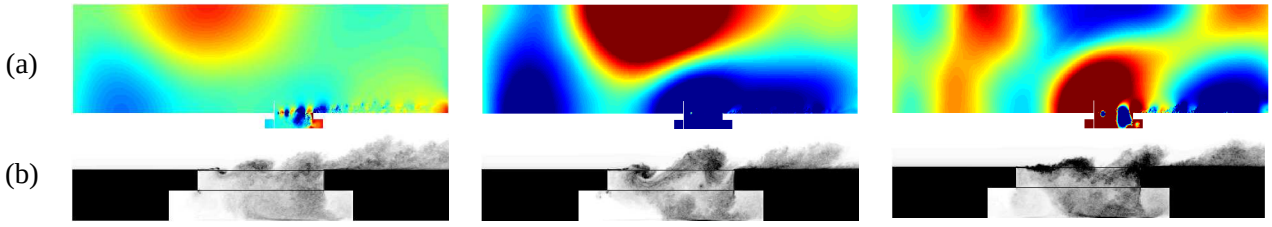

$M = 0.13$ $M = 0.18$ $M = 0.23$

Figure 2: Ducted cavity flow at several Mach numbers; instantaneous results: (a) pressure fluctuations in the duct (< 100 Pa), (b) spanwise average vorticity modulus in the cavity.

The ducted cavity considered here is partially covered as shown in Figure 1 where $d = 0.05$ m, $h = 0.02$ m, $H = 0.137$ m, and $L = 0.073$ m. For this configuration, RMs are given with $\alpha = 0.25$ and $1/\kappa = 0.57$ in equation (2). Experiments give the following results: lock-in occurs at $M = 0.13$ between RM3 and

DM1, at $M = 0.18$ between RM2 and DM1 and at $M = 0.23$ between RM3 and DM2. A preliminary LES using the previous algorithm with coincident grids have been carried out [20]. The lock-in phenomenon and the corresponding frequencies have been retrieved. However the amplitude of RMs was not well resolved. We hope that the overset-grid strategy makes it possible to improve the numerical results thanks to the mesh refinement in sensitive zones as the shear layer region where fine turbulent fluctuations can play a crucial role. Figures 2 show the instantaneous pressure field in the duct and spanwise average vorticity modulus in the cavity obtained by LES for $M = 0.13$, $M = 18$ and $M = 0.23$. At $M = 0.13$, the lock-in between RM3 and DM1 is well retrieved since three vortices are present in the shear layer. At $M = 0.18$, the lock-in between RM2, two vortices in the shear layer, and DM1 is also retrieved. At $M = 0.23$, the lock-in between RM3, three vortices in the shear layer, and DM2 is less matched, but appears in a more evident way than in Emmert *et al.* [20].

4 LES of a transonic flow in a sudden enlargement

Strong interactions between shock oscillations, internal aerodynamic noise and acoustic duct modes are often observed in confined flows and may be a source of undesirable vibrations or fatigue for structures. A transonic flow passing a sudden expansion in a duct is studied in this section. This kind of flow can be found downstream control devices such as valves encountered in power plants pipe systems . The flow in the nozzle throat is ex-

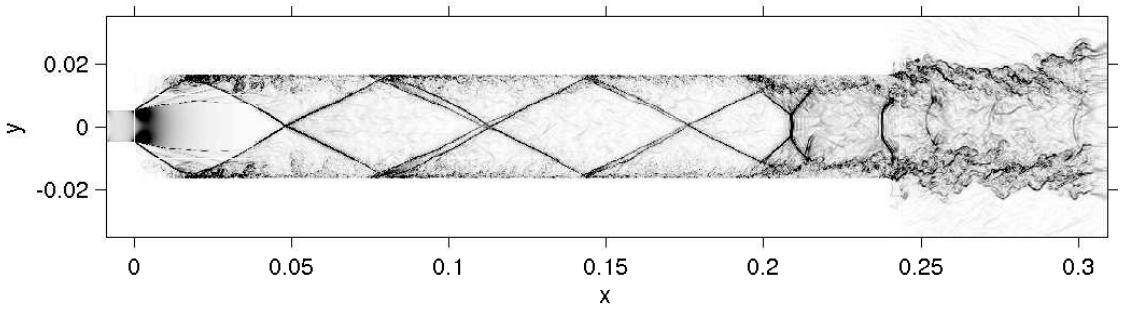

Figure 3: Sudden expansion of a transonic flow for pressure ratio $\tau = 0.15$: instantaneous numerical Schlieren $||\nabla\rho||$

panded abruptly when entering the expansion duct of larger cross-section. Different transonic and supersonic flow regimes have been investigated as a function of the pressure ratio τ defined as $\tau = p_{\text{outlet}}/p_{\text{inlet}}$. For very low pressure ratio, the flow is entirely supersonic. An instantaneous snapshot of the density gradient modulus represented in Figure (3). A system of crossing oblique shock waves is observed as in the experiments. In addition, shocks interact with the boundary layers developing at the walls of the expansion duct. The shock waves are reflected on the lower and upper wall respectively and form a symmetrical cell structure. The boundary layers significantly thicken at the shock reflection. Others flow regimes have been studied in Ref. [20]. Increasing the pressure ratio, the oblique shock wave system disappears and the supersonic expansion ends up behind a single normal shock. In this case a strong coupling between the self-sustained oscillations of the normal shock and the longitudinal acoustics modes of the duct is observed as in the experiments. For higher pressure ratios, the flow is asymmetric and exhibits shock cells.

5 Rod-airfoil interaction

Rod-airfoil configurations are believed to be a benchmark well-suited for numerical modeling of sound generation processes in turbomachines [21]. As shown in Figure 4, the impingement of the vortical structures

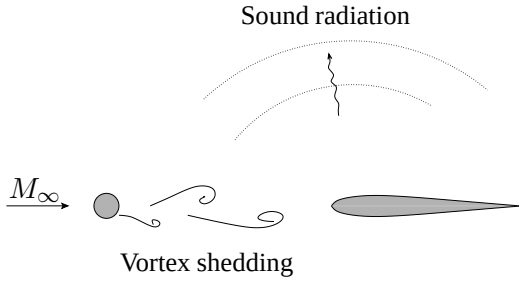

Figure 4: Sketch of the sound generated by an airfoil interacting with the wake of a rod, placed in an uniform flow with a free-stream Mach number M_∞.

in the wake of the cylinder on the leading edge of the airfoil generates sound sources. Several attempts have already been made to investigate rod-airfoil flow configurations by means of numerical simulations via hybrid approaches [22, 23]. The direct noise calculation of this phenomena *via* LES is investigated in the present section.
The calculation aims at reproducing the features of the aerodynamic and acoustic measurements performed by Jacob *et al.* [21]. The flow configuration is a symmetric NACA0012 airfoil located one chord downstream a rod, whose wake contains both tonal and broadband fluctuations. The airfoil chord is equal to $c = 0.1$m and the rod diameter d is taken to be a tenth of the chord length. The free-stream Mach number M_∞ is 0.2 so that the Reynolds numbers based on the chord length and the rod diameter are respectively given by $Re_c = 5 \times 10^5$ and $Re_d = 5 \times 10^4$.
As an illustration, an instantaneous snapshot of the magnitude of the velocity field, taken in the central plane of the computational domain, is presented in Figure 5. It is seen that turbulence ignition is achieved by the

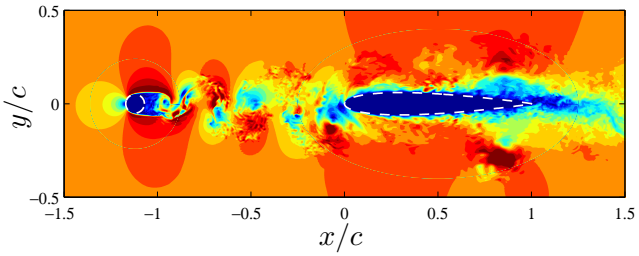

Figure 5: Snapshot of the magnitude of the velocity field in the central plane of the computational domain. The rod and the airfoil boundaries are represented by the dashed white lines. Colorscale from 0 m.s^{-1} (blue) to 100 m.s^{-1} (red).

rod. In particular, large scale organized structures are observed in its wake and correspond to periodic vortex shedding. Smaller turbulent scales are furthermore visible.

6 Conclusion

High-order algorithms are now matured for performing LES of compressible flows. The use of high-order interpolation in suitable overset-grid strategies makes it possible to study realistic applications. In addition, applying non-linear filter with improved shock detectors introduces numerical dissipation only within shock region without damaging the spectral-like accuracy in the rest of the computational domain. With such numerical procedure, three realistic configurations have been studied in this paper. In this three cases, the aeroacoustic coupling is retrieved.

The extension of moving meshes is in progress [24]. A special attention concerning the free-stream preservation must be paid. In practice, corrective non-conservative terms are employed as in [5]. In addition, it is well known that the use of explicit time integration can be time-consuming in particular for low-speed flows because the physics scales are driven by the convection wave and not by the acoustic ones. The use of implicit time integration makes it possible to overcome the problem linked to the restrictive explicit stability constraint without damaging turbulent fluctuations using a suitable time step [15, 25].

Acknowledgments

This work is supported by the “Agence Nationale de la Recherche” under the reference ANR-06-CIS6-011. The authors want to thank Dr. Bill Henshaw for his useful advices concerning the overset strategy.

References

[1] Colonius T. and Lele S. K. Computational aeroacoustics: progress on nonlinear problems on sound generation. Prog. Aerospace Sci., 40, 345–416, 2004.

[2] Lele S. K. Compact finite difference schemes with spectral-like resolution. J. Comp. Phys., 103(1), 16–42, 1992.

[3] Tam C. K. W. and Webb J. C. Dispersion-Relation-Preserving Finite Differences Schemes for Computational Acoustics. J. Comp. Phys., 107(2), 262–281, 1993.

[4] Bogey C. and Bailly C. A family of low dispersive and low dissipative explicit schemes for flow and noise computations. J. Comp. Phys., 194(1), 194–214, 2004.

[5] Visbal M. R. and Gaitonde D. V. On the Use of Higher-Order Finite-Difference Schemes on Curvilinear and Deforming Meshes. J. Comp. Phys., 181(1), 155–185, 2002.

[6] Marsden O., Bogey C., and Bailly C. High-order curvilinear simulations of flows around non-Cartesian bodies. J. Comput. Acoust., 13(4), 731–748, 2005.

[7] Delfs J. W. An overlapped grid technique for high resolution CAA schemes for complex geometries. AIAA Paper 2001-2199, 2001.

[8] Sherer S. E. and Scott J. N. High-order compact finite-difference methods on general overset grids. J. Comp. Phys., 210(2), 459–496, 2005.

[9] Desquesnes G., Terracol M., Manoha E., and Sagaut P. On the use of a high order overlapping grid method for coupling in CFD/CAA. J. Comp. Phys., 220(1), 355–382, 2006.

[10] Garnier E., Mossi M., Sagaut P., Comte P., and Deville M. On the use of the shock-capturing schemes for Large-Eddy Simulation. J. Comp. Phys., 153(2), 273–311, 1999.

[11] Garnier E., , Sagaut P., and Deville M. A Class of Explicit ENO Filters with Application to Unsteady Flows. J. Comp. Phys., 170(1), 184–204, 2001.

[12] Bogey C., de Cacqueray N., and Bailly C. A shock-capturing methodology based on adaptive spatial filtering for high-order non-linear comptations. J. Comp. Phys., 228(5), 1447–1465, 2009.

[13] Daude F., Emmert T., Lafon P., Crouzet F., and Bailly C. A high-order algorithm for compressible LES in CAA applications. AIAA Paper 2008-3049, 2008.

[14] Bogey C. and Bailly C. Large eddy simulations of transitional round jets: influence of the Reynolds number on flow development and energy dissipation. Phys. of Fluids, 213(2), 777–802, 2006.

[15] Rizzetta D. P., Visbal M. R., and Blaisdell G. A. A time-implicit high-order compact differencing and filtering scheme for large-eddy simulation. Int. J. Numer. Methods Fluids, 42, 665–693, 2003.

[16] Rowley C. W. and Williams D. R. Dynamics and control of high-Reynolds number flow over open cavities. Annu. Rev. Fluid Mech., 30, 251–276, 2006.

[17] Rossiter J. E. Wind-tunnel experiments on the flow over rectangular cavities at subsonic and transonic speeds. Aeronautical Research Council Reports and Emoranda, pages –, 1964.

[18] Stanek M. J., Visbal M. R., Rizzetta D. P., Rubin S. G., and Khosla P. K. On a mechanism of stabilizing turbulent free shear layers in cavity flows. Comput. Fluids, 36(10), 1621–1637, 2007.

[19] Comte P., Daude F., and Mary I. Simulation of the Reduction of the Unsteadiness in a Passively-Controlled Transonic Cavity Flow. J. Fluids Struct., 24(8), 1252–1261, 2008.

[20] Emmert T., Lafon P., and Bailly C. Computation of Aeroacoustic Phenomena in Subsonic and Transonic Ducted Flows. AIAA Paper 2007-3429, 2007.

[21] Jacob M. C., Boudet J., Casalino D., and Michard M. A rod-airfoil experiment as benchmark for broadband noise modeling. J. theoret. Comput. Fluid Dyn., 19(3), 171–196, 2005.

[22] Boudet J., Grosjean N., and Jacob M. C. Wake-airfoil interaction as broadband noise sourceÂ : a large-eddy simulation study. Int. J. Aeroacoustics, 4(1), 93–116, 2005.

[23] Greschner B., Thiele F., Jacob M. C., and Casalino D. Prediction of sound generated by a rod-airfoil configuration using EASM DES and the generalised Lighthill/FW-H analogy. Comput. Fluids, 37(4), 402–413, 2008.

[24] Daude F., Lafon P., Crouzet F., and Bailly C. An Overset-Grid Strategy for Aeroacoustics and Aeroelasticity of Moving Bodies. Fluid-Structure Interaction. Theroy, Numerics and Applications, pages 283–294, 2008.

[25] Daude F., Mary I., and Comte P. Implicit time integration method for LES of complex flows. In Direct and Large-Eddy Simulation VI, pages 771–778. Springer, 2006.